Assessment and control of active impedances for modern antenna arrays

Joni Lappalainen[1], Jaakko Juntunen[1] and Jussi Rahola[1]

[1]Optenni Ltd, Finland

Introduction

Forthcoming 5G networks impose new kind of challenges to RF designers. The bandwidths available at traditional frequencies are insufficient as both the number of users and the requirements for data rates are increasing. The natural option is to move to higher frequencies, but this comes at a cost. The well-known Friis free-space path loss formula gives the ratio of received (P_r) and transmitted power (P_t) as a function of the wavelength, array separation d and gains G_t and G_r of the transmitting and receiving antennas:

$$\frac{P_r}{P_t} = G_t G_r \left(\frac{\lambda}{4\pi d}\right)^2$$

From the formula, one easily recognizes that increasing frequency will result in less received power for fixed antenna gains. If the same amount of power is to be delivered at 20 GHz and 3 GHz, the efficiency of the 20 GHz system would have to be approximately 16 dB higher. As we know, this is unachievable. However, for now we have considered a fixed directivity for the antennas, whereas in reality the directivity D of an antenna is related to its effective aperture area A_{eff}, which is also a function of frequency:

$$A_{eff} = \frac{\lambda^2}{4\pi} D$$

This means that the operation of the link can be restored or even improved by retaining the physical size of the antenna as the frequency increases, resulting in more directivity. However, as the directivity increases, the beam of the device gets narrower. A practical solution is to use *antenna arrays* instead of electrically large antennas. The directivity of the system is then achieved by increasing the number of elements and introducing *beamforming*, i.e. summation of the element patterns [1].

Traditional arrays consisting of well-isolated elements are usually studied via analytical beamforming techniques most suitable to quasi-infinite arrays of hundreds of elements. However, to achieve the required ~16-20 dB improvement compared to the 4G systems, some 20-60 elements are typically enough. We foresee that a new generation of antenna arrays will emerge, exhibiting some combination of the following attributes: (a) planar, low-cost structures suitable for mass production (b) compact size (c) operating frequencies in tens of GHz (d) dynamic beam steering (e) tight integration with integrated circuits (ICs) [2]. These attributes lead to a design challenge that is characteristic of this class of antenna arrays, namely the handling of the *active impedance* or *active reflection coefficient* (ARC) of antenna element. In contrast to classical port input impedance definition where the signal reflection is due to the excitation at the port itself, while all other ports are terminated at 50 Ohm load, the active impedance accounts for the coupling from the simultaneous excitation of all ports. If there is finite isolation between the antenna elements, some power of the neighboring elements is coupled to the port under observation, and these coupled signals interfere with the reflected signal – constructively or destructively – causing the apparent impedance of the port to change.

There are two key observations regarding the active impedance: first, when the isolation between the antenna elements becomes poorer, the variation in the active impedance becomes larger; second, the active impedance depends on the excitation vector. This means that the active beam steering dynamically changes the load

impedance of the power amplifiers driving the array. This in turn changes the gain and efficiency of the amplifiers, which must be accounted for while designing the beam steering strategy. Hence beamforming optimization for finitely isolated arrays needs to consider the individual element patterns, system S-parameters, varying impedance matching, active reflection coefficients and amplifier characteristics simultaneously, all of which are beyond the scope of analytical beamforming techniques.

Electromagnetic limits of arrays

To briefly recap, an array is a group of antennas that are fed simultaneously by a single or multiple feeding ports to form a beam that differs significantly from the element pattern(s) of the elements within the array. Typical reasons to use arrays include beam steering, mitigation of interference (null creation) and the increase of directivity.

Traditionally, the performance of the array is determined by its electromagnetic operation, i.e. properties of the beam are assessed independently of the circuit properties. An example of a traditional beam property is the *beam scanning range* of an array, describing the maximum attainable gain to any given direction. This is heavily related to the isolated element pattern of the array elements, but there is often significant contribution from the coupling effects to the neighboring elements, resulting in for example scan blindness [3-4]. The beam scanning range illustrated in Figure 1 is calculated with Optenni Lab RF Design Automation Platform, taking into account not only the individual element patterns for each of the array elements but also the coupling effects for each feed vector through the S-parameter matrix [5].

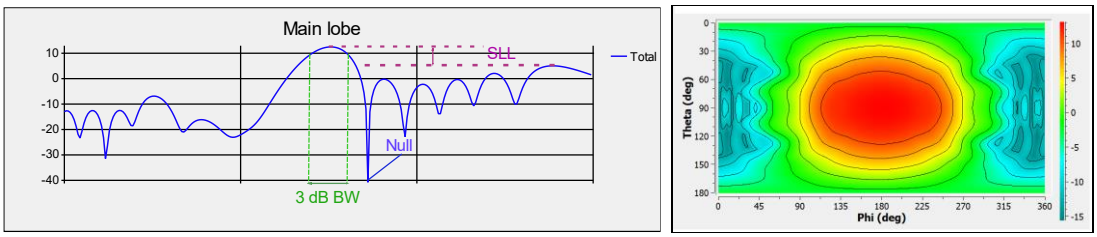

Figure 1: (Left) A 2D-cut of a radiation pattern, illustrating the side lobe level (SLL), 3 dB beam width, nulls, as well as main lobe direction. (Right) 2D-colormap of the beam scanning range, i.e. attainable maximum gain to any given direction of a 18x1 patch antenna array (broadside direction is given by Phi = 180, Theta = 90).

Impedance detuning and ARC maxima as a function of beam direction and amplitude tapering

Let's first consider a 6x6 patch antenna array operating at 28 GHz, exhibiting 24 dB matching level and 14 dB of isolation between neighboring elements, sketched in Figure 2. We have studied 2D-beamsteering scheme in which for a given beam steering angle α from broadside, the beam direction is revolved full circle around the broadside direction as illustrated in Figure 2. As mentioned earlier, ARCs are known to be strong functions of inter-element isolation, desired beam direction and amplitude tapering. However, the question remains: how much is much, i.e. when should one expect trouble?

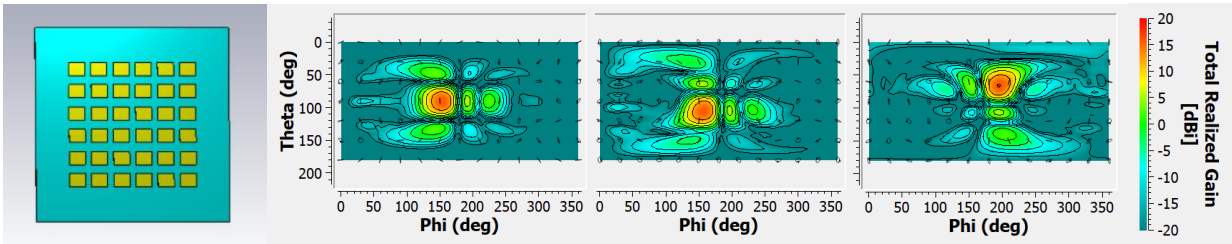

Figure 2: The 6x6 patch array geometry on the left, and 2D color plots of its radiation pattern for a few beam direction samples corresponding to beam steering angle $\alpha = 30°$. Here the broadside direction points towards Phi = 180, Theta = 90. The plots are calculated with the RF Design Automation Platform used throughout this study.

We steered the beams in cones around the broadside direction (corresponding to a given beam steering angle) and recorded the worst case ARC over the ports and the beam directions. Furthermore, in Figure 3. we run the study using uniform excitation and a few Dolph-Chebyshev amplitude tapering schemes. Albeit this array exhibits an isolation level considered poor by most array designers, it seems that with uniform excitations, denoted as D-C = 0, the ARC is only a weak function of the steering angle. However, as the amplitude tapering increases, i.e. the dynamic range of amplitude between the neighbouring elements is increased, the ARC maximas start to quickly deteriorate. It also appears that the larger the beam steering angle, the quicker the results deteriorate as a function of the amplitude tapering.

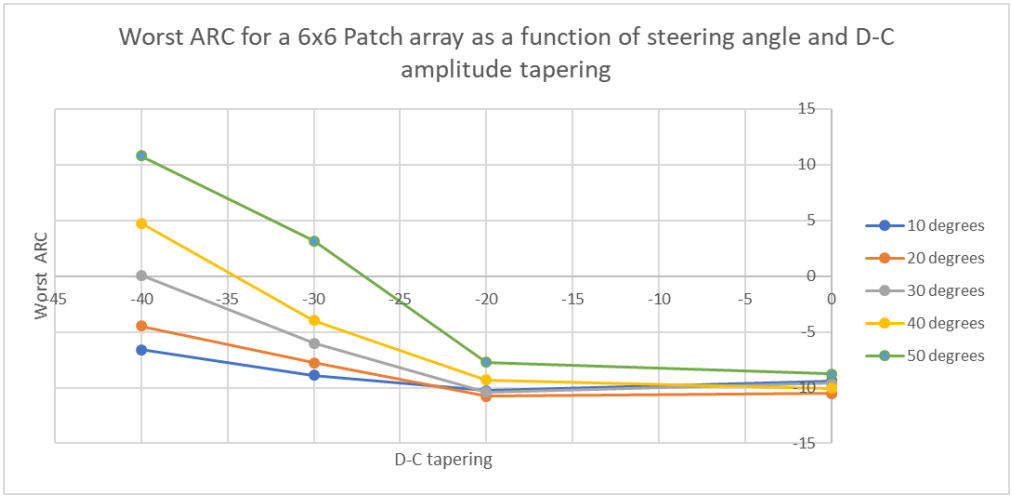

Figure 3: Worst-case magnitude of the ARC as a function of the Dolph-Chebyschev (D-C) side lobe level parameter for different beam steering angles α. For each α, the maximum magnitude of ARC over the ports and beam directions is recorded.

The study was then replicated to a larger copy of the same array in 8x8 constellation, i.e. with 78% more elements. Perhaps surprisingly, the previous findings were found to hold true: with more than -20 dB D-C tapering the ARCs deteriorated quickly as a function of the steering angle.

ARCs on the Smith chart for different beam steering directions and tapering

For now, we have only considered the magnitude of the worst ARC over the ports and beam directions for a set of beams corresponding to a given beam steering angle α. Any RF engineer knows that there is significantly more information embedded on the Smith chart compared to a plain magnitude value. Based on a number of different antenna array designs we have observed an interesting and practically useful array property, which appears to be almost universally applicable:

The simultaneous excitation of the array elements moves the active reflection coefficients *averaged over the ports* to a location on the Smith chart, *which is independent of the beam direction*, up to a critical steering angle with respect to broadside.

The above statement deserves some elaboration. First, the ARC of any individual port does depend upon the beam steering direction, but the ARCs of all ports are centered at nearly the same location in Smith chart. Second, the ARCs get worse as a function of steering angle from the broadside, but, again, they are approximately centered around the same point. Figure 4 illustrates the phenomenon for a sample 6x6 array. The observation leads to a very important conclusion: *one can improve the ARC behavior by considering the broadside excitation only.* If we can match the antenna for broadside ARCs, the above implies that the ARCs are improved for any other beam direction as well compared to the case where the antennas would have been perfectly 50 Ohms.

Therefore, for arrays with less-than-perfect isolation, it is really beneficial to check the broadside ARCs. It may come as a surprise that the port impedances that are designed nearly ideal in S-parameter sense can get detuned dramatically upon broadside excitation. In other words, going from unit element design into coupled array context, first, the input impedance of an antenna element is detuned by the presence of the other elements, and second, the active input impedance differs from the input impedance, and depends on the excitation.

From the array design perspective this means that the ARCs must be considered early in the design cycle. It is mostly wasted effort to spend lots of time trying to design the unit element geometry such that it provides an excellent input impedance by itself or when combined into the desired array grid, as the input impedance gets detuned anyway by the simultaneous excitation of the ports. A better figure of merit according to our research is the ARC related to a broadside excitation. One can use a simple matching circuit to correct the designed unit element's impedance such that it provides the optimal impedance to the PA when combined into an array *and* excited with a uniform excitation vector.

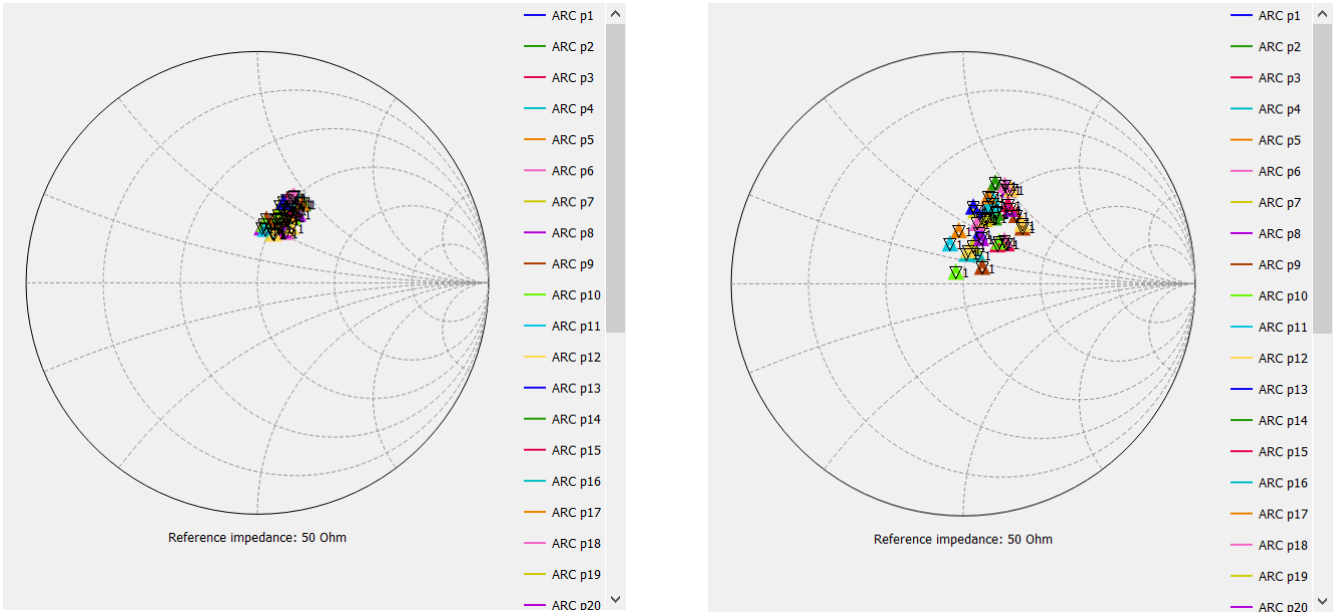

Figure 4. ARCs of a sample 6x6 array due to uniform broadside excitation (left) and due to 30° beam steering off the broadside (right). The center point of the ARCs is almost at the same position in Smith chart.

Let us provide evidence and examples of our hypothesis that the average ARC is independent of the beam direction. We use a 60 GHz patch antenna array as the design prototype, and we have created two EM model variants of it using CST Microwave Studio: "full size and "dense", depicted in Figure 5. The radiator is identical in both cases, but they are packed in a sparser and a denser configuration.

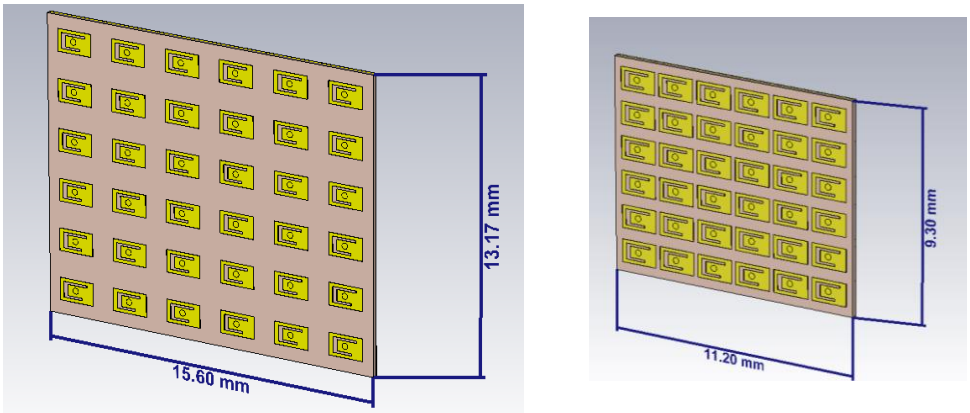

Figure 5. Example patch array designed for 60 GHz operation. "Full-size" on the left and "dense" on the right. All radiator elements are identical. The element separation for full size array is 2.6 mm along the x-axis and 2.2 mm along the y-axis; for dense array the separations are 1.8 mm and 1.5 mm, respectively. The isolation level is about 19 dB for the full-size array and 14 dB for the dense array.

In Figure 6 we show the S_{nn} and ARCs due to broadside excitation vector for the arrays. No matching circuits are employed at this point. We can see that the dense array shows larger S_{nn} detuning and larger spread of the ARCs than the full-size array.

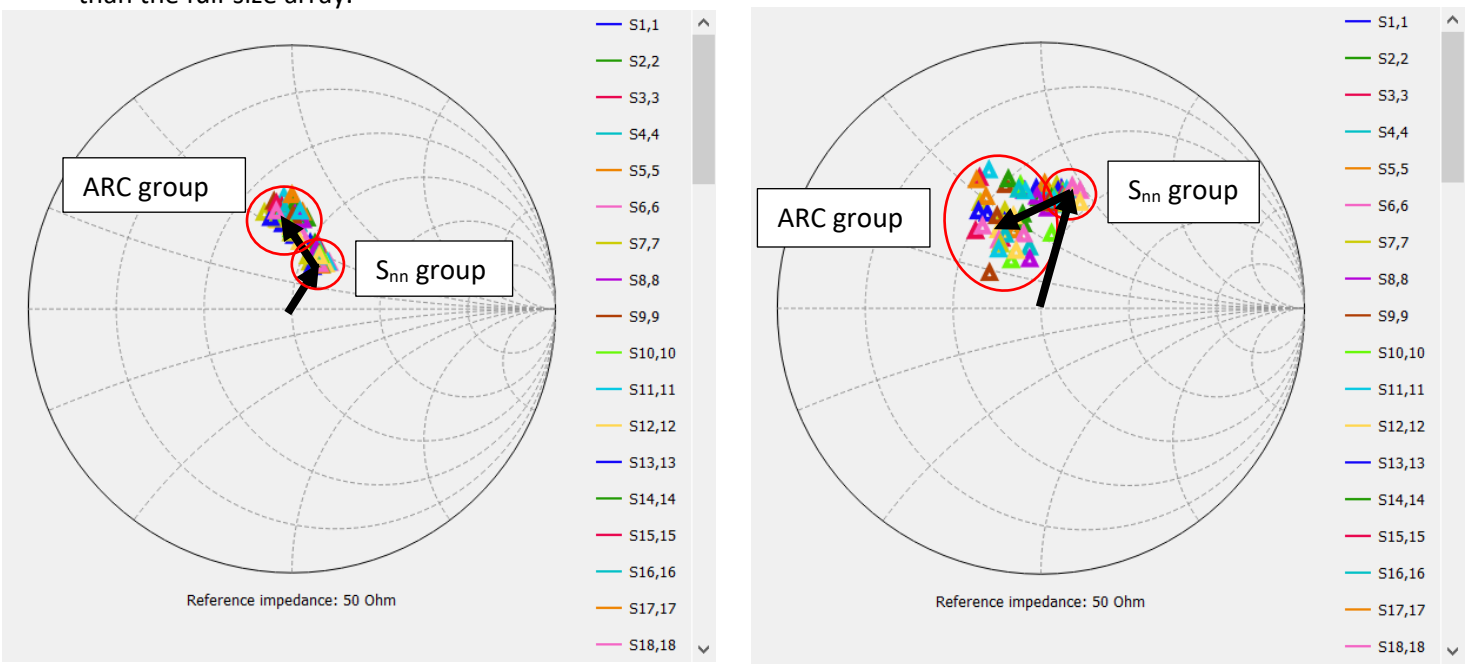

Figure 6. S_{nn} and ARCs due to broadside excitation. Full size array on the left and dense array on the right. The black arrows depict the impedance detuning due to power loss through port coupling, and active impedance detuning due to signal coupling.

Similar to the study above, in reference to Figure 2, we have carried out a 2-dimensional beam scanning analysis where the beam steering angle α is again progressively increased, and for each α the beam direction is rotated a full circle around the broadside direction. For every beam direction, ARCs for all ports are calculated, and their

average over the ports is plotted on the Smith chart. Figure 7 shows the trajectories so formed. A zoom-in shows the weak dependence of the center point of the ARCs on the beam direction.

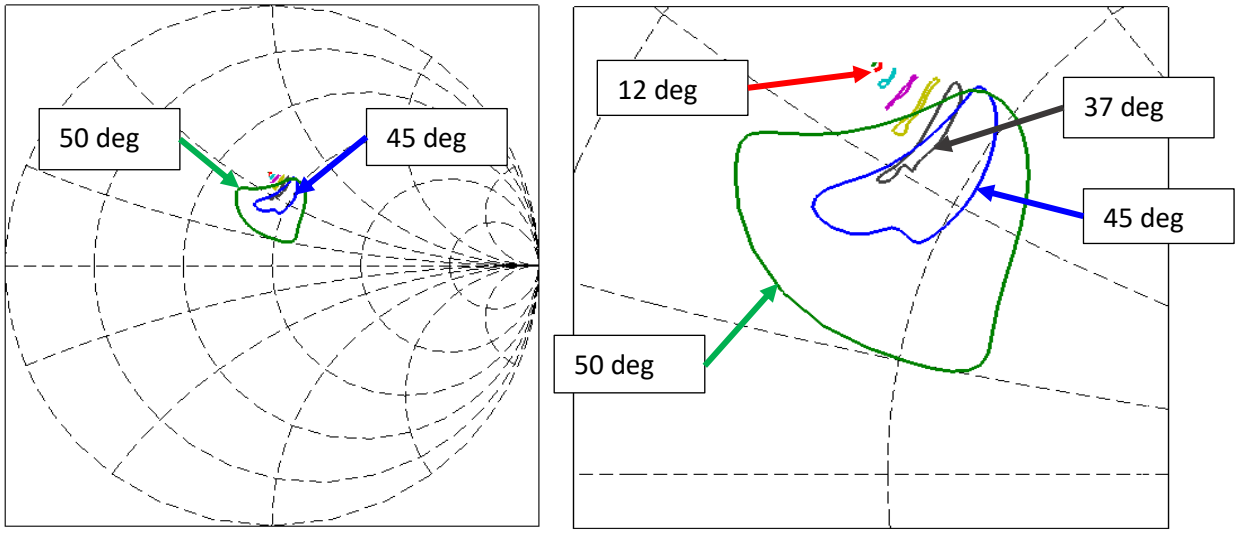

Figure 7. Trajectories of the average ARC over ports, formed by rotating the beam direction around the broadside direction for a number of constant steering angles α for the full-size array. Uniform amplitude tapering is applied. For all beam directions corresponding to steering angles of up to about 45 degrees, the average ARC over the ports is almost independent on beam direction.

If we consider the dense array instead, and carry out similar analysis, we now have a different plot with more variation (Figure 8), but in fact the same conclusion holds: for sufficiently small steering angles the average ARC over the ports is essentially fixed, in this case up to a steering angle of about 32 degrees.

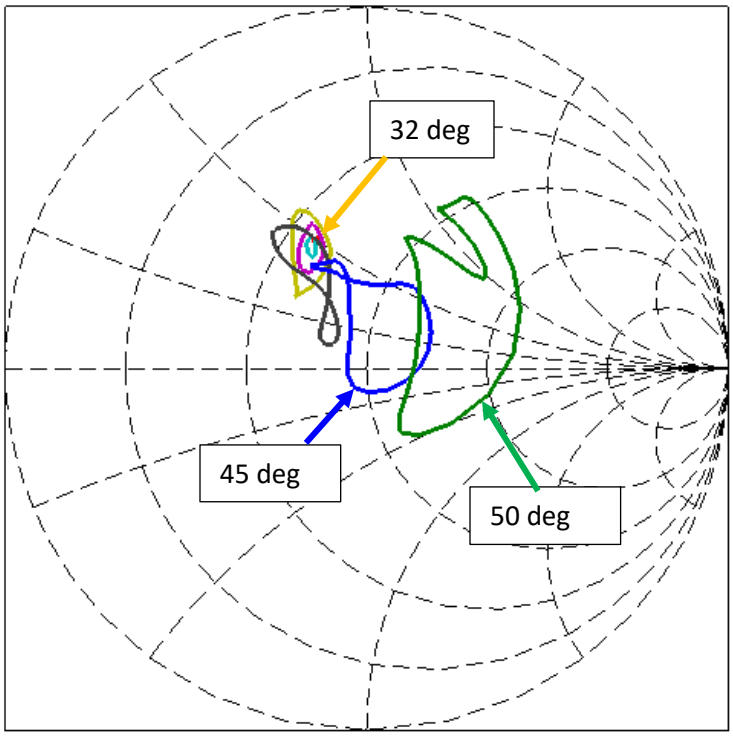

Figure 8. Average ARC over ports for the dense array as a function of beam steering angle. Uniform amplitude tapering is applied. This time the average ARC over ports is nearly constant up to a beam steering angle of 32 degrees.

To summarize, one can thus optimize the array for ARCs by adjusting the array element impedances such that the average ARC over the ports and for broadside excitation is in the middle of the Smith chart (or at the PA load-pull gain/efficiency optimum). In the study above we have assumed uniform amplitude tapering. We tested amplitude tapering effect by applying a Dolph-Chebyshev excitation with sidelobe level parameter ranging from -15 dB to -25 dB, and with the studied arrays the conclusion is still valid. Increasing amplitude taper causes ARCs to worsen as observed before, but, remarkably, the average ARC over the ports for small enough beam steering angles is essentially independent also on the amplitude taper. An extreme example is depicted in Figure 9 for the dense array and -25 dB sidelobe level parameter, showing no much difference to the Figure 8 for steering angles up to about 25 degrees.

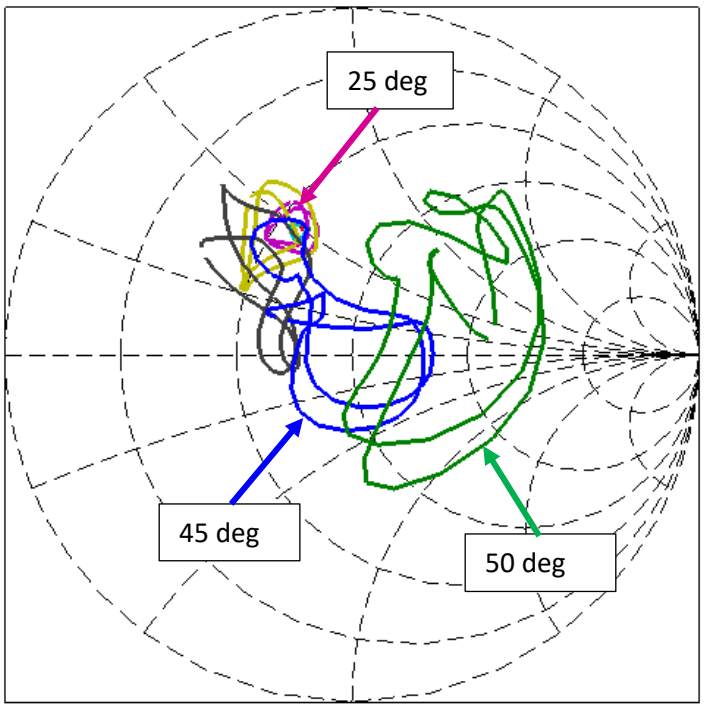

Figure 9. Average ARC over ports for dense array as a function of the beam steering angle. Strong amplitude tapering with -25 dB sidelobe level parameter in Dolph-Chebyshev excitation scheme is applied.

Performance improvement due to ARC matching

We will finally consider the benefits of the proper ARC matching as outlined above to a practical case. We consider the same full size and dense arrays, matched to either good S_{nn} or good broadside ARC, and employ a 60 GHz IC amplifier model prematched to 50 Ohms for each antenna element. The ARC causes some gain degradation of the amplifiers, leading to degradation of array gain.

We excite the array by excitation vectors with moderate amplitude tapering to reduce side lobes (Dolph-Chebyshev sidelobe parameter -20 dB), and with steering angles from 0° to 60° from broadside. The main lobe is rotationally symmetric with a 3 dB beamwidth of about 20°. Figure 10 shows the realized main lobe gain as a function of the steering angle. We can see two interesting things: (1) matching to broadside ARC leads to an

improvement of the gain especially for the dense array and larger steering angles, where a 0.5-0.6 dB improvement is achieved for steering angles 50-60°. (2) the gain for the dense array is considerably flat, and in fact outperforms the full-size array's gain beyond about 48° steering angle. Incidentally, for the excitation scheme used, the sidelobe level for the full-size array is higher than the main lobe level for these larger steering angles, whereas the sidelobe level for the dense array is -9 dB still at 60° steering angle. The sidelobes of the full-size array are effectively identified as grating lobes emerging from a slightly larger than $\lambda/2$ separation along the x-axis.

The conclusion is that the broadside ARC matching is especially useful for dense arrays with the aim of wide steering angle. The ARC matching can be absorbed in the IC amplifier output matching section. The 0.6 dB performance improvement translates to 7% longer range or 13% reduced TX power or about ±5° wider useful beam scan angle for the same array geometry.

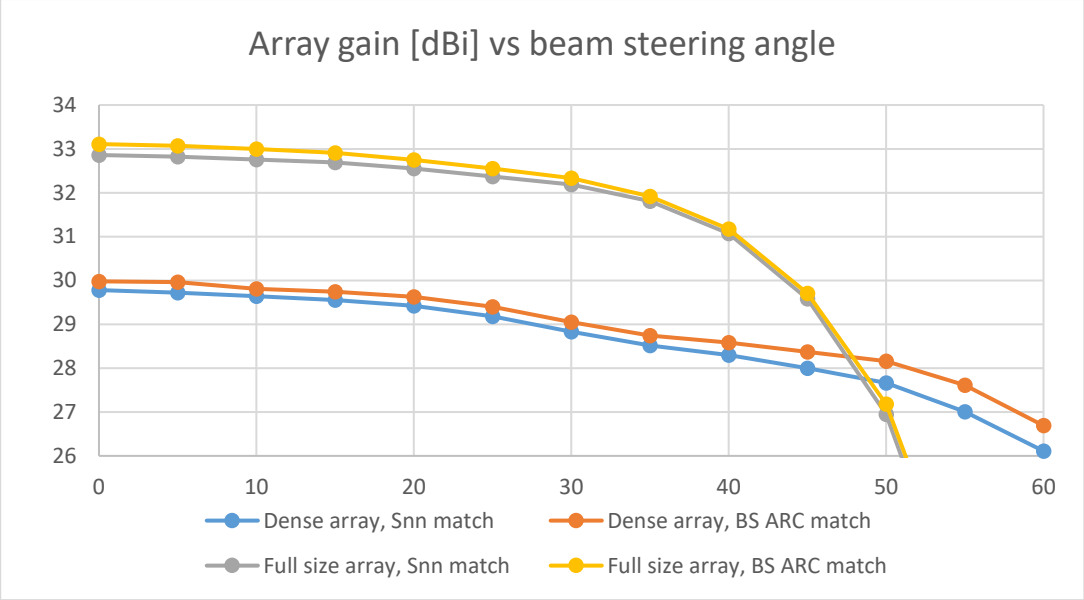

Figure 10. Array gain as a function of the beam steering angle α with respect to broadside, for both dense and full-sized arrays with traditional and broadside ARC-matched array elements.

Conclusions

The emerging 5G infrastructure calls for new kinds of designs from antenna engineers. Due to the large required operation bandwidths of the arrays the designers must deal with sub-optimal array element spacing and isolation levels. In this new environment the accurate co-simulation of the EM and circuit properties of antenna arrays becomes increasingly important. However, it was found that the EM and circuit design challenges are partially independent and that the worst-case ARC does not depend much on the number of elements in the array. This allows for a quick and efficient ARC analysis of larger arrays by utilizing scaled-down models.

For non-perfectly isolated arrays a straightforward design methodology has been introduced that results in improved operation when compared to a traditional, impedance-wise perfectly matched array. This methodology is based on the finding that the ARCs are located in a well-defined region of the Smith chart for practical steering angles and amplitude tapering schemes. The average ARCs over ports can be matched with a

simple matching circuitry that can be implemented directly in the IC's matching circuitry or in the feed network of hybrid beamforming devices.

To truly understand the applicability and limitations of our research, some additional studies should be conducted on the limitations of the proposed scaled-down assessment of ARC behavior for large arrays. Furthermore, the proposed broadside matching scheme should be further tested with arrays with varying isolation levels, inter-element spacings and element types.

[1] W. Roh *et al*., "Millimeter-wave beamforming as an enabling technology for 5G cellular communications: theoretical feasibility and prototype results," in *IEEE Communications Magazine*, vol. 52, no. 2, pp. 106-113, Feb. 2014.

[2] B. Sadhu, X. Gu and A. Valdes-Garcia, "A survey of Silicon-Based mm-Wave Phased Arrays Using Multi-IC Scaling", in IEEE microwave Magazine, vol 20, no. 12, pp. 32-49, Dec. 2019.

[3] D. M. Pozar and D. H. Schaubert, "Scan blindness in infinite phased arrays of printed dipoles", IEEE Trans. Antennas Propag., vol. 32, no. 6, pp. 602–610, Jun. 1984.

[4] E. Adas, F. De Flaviis and N. G. Alexopoulos, "Realization of Scan Blindness Free Finite Microstrip Phased Arrays Based on Mode-Free Radiating Electromagnetic Bandgap Materials," in IEEE Trans. Antennas Propag., vol. 66, no. 7, pp. 3375-3382, Jul. 2018.

[5] https://www.optenni.com/